Number and intrinsic activity of cobalt surface sites in platinum promoted zeolite catalysts for carbon monoxide hydrogenation

Alexandre Carvalho, Vitaly Ordomsky, Nilson Marcilio, Andrei Khodakov

Catalysis Science & Technology

Accepted Manuscript

This article can be cited before page numbers have been issued, to do this please use: A. Carvalho, V. Ordomsky, N. Marcilio and A. Khodakov, *Catal. Sci. Technol.*, 2020, DOI: 10.1039/C9CY02421B.

ROYAL SOCIETY OF CHEMISTRY

rsc.li/catalysis

Catalysis Science & Technology

View Article Online
DOI: 10.1039/C9CY02421B

ARTICLE

Number and intrinsic activity of cobalt surface sites in platinum promoted zeolite catalysts for carbon monoxide hydrogenation

Received 00th January 20xx,
Accepted 00th January 20xx

DOI: 10.1039/x0xx00000x

Alexandre Carvalho[a,b], Vitaly V. Ordomsky[a], Nilson R. Marcilio[b] and Andrei Y. Khodakov[a*]

Supported cobalt catalysts are the catalysts of choice for synthesis of paraffinic hydrocarbons from carbon monoxide and hydrogen. In this paper, the number and intrinsic activity of cobalt nanoparticles promoted with Pt localized in zeolites with different structure and pore diameter (ZSM-5, MOR and BEA) have been investigated by steady state isotopic kinetic analysis (SSITKA) under the conditions favouring higher methane selectivity. Promotion with Pt resulted in higher number and higher reactivity of surface intermediates leading to methane. The cobalt catalyst supported by MOR zeolite displayed the highest SSITKA reaction rate in carbon monoxide hydrogenation, followed by Co supported on BEA and in the last for Co supported on the zeolite ZSM-5. Good dispersion of cobalt nanoparticles inside and outside of the surface of MOR and BEA zeolites led to higher number of active sites. On the other hand, poor dispersion of cobalt nanoparticles on the external surface of ZSM-5 resulted in lowest intrinsic catalytic activity and lowest number of active sites. The intrinsic active of cobalt sites was however, almost unaffected by the inclusion of cobalt nanoparticles in the zeolite pores.

Introduction

Catalysts with supported cobalt nanoparticles are the catalysts of choice for low temperature Fischer-Tropsch (FT) synthesis, which produces middle distillates and waxes from syngas. The reaction occurs over supported metal nanoparticles, which provide active sites for carbon monoxide hydrogenation. The catalytic performance of cobalt catalysts in FT synthesis can be affected by several parameters such as promotion, cobalt nanoparticle size and cobalt localisation within the porous support.

It is known that the use of noble metals as promoters leads to a significant increase in FT catalytic activity[1] in both slurry and fixed bed reactors[2–4]. Pt as a promoter for cobalt FT catalysts supported on alumina and silica has been demonstrated a strong effect on the FT reaction rate[5,6]. Pt can produce several effects on the catalyst structure and performance[1]. Among them is better cobalt reducibility [7], which is due to lower activation energy to form the cobalt metallic phase from cobalt oxide in the presence of Pt[5].

The influence of the support on FT catalyst can be also important, once the support may significantly modify cobalt particle size, metal–support interactions, support acidity, porosity and mass transfer limitations[5,8]. Silica, alumina, titania and zeolites are common commercial supports for cobalt FT catalysts [9–12]. Syngas conversion over metal-zeolite catalysts involves bifunctional catalysis, where CO hydrogenation occurs on metal sites, while the zeolite could perform hydrocarbon cracking and isomerization under the conditions of FT synthesis [13,14].

Transient kinetic methods including the steady state isotopic transient kinetic analysis (SSITKA) are powerful techniques for the kinetic investigation of heterogeneous catalytic reactions at molecular level. SSITKA addresses measuring the transient response of isotopic labels in the reactor following an abrupt change (switch) in the isotopic composition of one of the reactants. Only isotopic composition of the feed is changed, while chemical composition remains the same [15]. SSITKA can be used to determine the number and intrinsic activity of active sites, site heterogeneity

[a] Univ. Lille, CNRS, Centrale Lille, ENSCL, Univ. Artois, UMR 8181 – UCCS – Unité de Catalyse et Chimie du Solide, F-59000 Lille, France.
[b] Department of Chemical Engineering, Federal University of Rio Grande do Sul, Porto Alegre, 90040-040, Brazil
*Corresponding author: andrei.khodakov@univ-lille.fr

DOI: 10.1039/C9CY02421B

and concentration of different types of adsorbed reaction intermediates,

surface residence time, activity distributions and site coverage [12,16,17]. In previous reports [18–25], SSITKA has been used to evaluate the effect of different promoters, support modification and cobalt particle size on the type, concentration and reactivity of the surface intermediates. For example, Rane[26] et al. found different concentrations of CO and CH_x intermediates on the cobalt catalysts supported by ɣ, Φ-, δ- and α-Al_2O_3. Vasiliades[27] et al. uncovered that the coverage, turnover frequency (TOF) and CH_x residence time slightly increased with increasing Co particle size (in the 7–10 nm range). The effect of the support on the SSITKA kinetic parameters was also observed by Kim Phan[28] et al. for cobalt catalysts supported on conventional and macroporous (MPS) alumina. The number of intermediates leading to methane (N_{CH4}) on cobalt supported on MPS-Al_2O_3 was higher (7.0 µmol/g) than that for Co/α-Al_2O_3 (4.1 µmol/g), while the Re promotion led to the increase in the number of CH_x intermediates to 11.3 µmol/g. This trend correlated with the reaction rate, which was higher for cobalt Re-promoted supported on MPS-$A_{l2}O_3$. The conclusions are in agreement with earlier results of Frøseth[29] et al. and Hanssen[30] et al. who observed an increase in the overall activity and in the concentration of active surface intermediates on the promotion with Pt and Re.

Catalytic performance of cobalt zeolite catalysts often depends on the type of zeolite. This effect can be attributed either to the variation of the number of active sites or to the modification of intrinsic site activity. Measuring the size of metal nanoparticles, number of metal active sites in zeolites and their intrinsic activity is usually a difficult task; the metal particles in zeolite micropores are often very small (<1 nm) and hardly visible by most of characterization techniques such as conventional TEM. Conventional chemisorption experiments are habitually conducted with freshly activated catalysts and under the conditions very different from those in the catalytic tests. Most of conventional steady state kinetic techniques cannot separate these two rather different phenomena responsible for modification of catalytic performance. SSITKA has a number of advantages compared to conventional characterization and kinetic methods. It can provide independent information on both the number of active species and their intrinsic reactivity.

The aim of this work is to evaluate the number of active sites and their intrinsic activity for CO hydrogenation over cobalt FT catalysts promoted with Pt and supported on MOR, BEA and ZSM-5 zeolites using SSITKA.

Results and discussion

Measuring the number of cobalt surface sites by SSITKA

All catalysts were activated in hydrogen flow of 8 mL/min at 400 °C with the temperature ramp of 5 °C/min. The Pt promoted cobalt catalysts supported on zeolites did not shown any visible deactivation during 12-14 h of the reaction. The reduction temperature of the cobalt supported on the zeolites was previously determined by Subramanian et al. [13] by temperature-programmed reduction with hydrogen (H_2-TPR). The TPR profiles exhibited a single group of peaks around 350-400 °C assigned to the reduction of cobalt oxide species to metallic phases. Subramanian et al. [13] also observed a decrease in the pore volume for zeolite BEA of around 50%, for MOR (around 20%) and for ZSM-5 (10%) after the introduction of about 20 wt. % of Co via impregnation. The surface area and pore volume of CoPt/ZSM-5 only slightly decreases after impregnation compared to other zeolites.

The 3D pore structure of BEA (0.76×0.64 nm) is more open than that of MOR (0.65×0.7 nm; 1 D) and ZSM-5 (approximately 0.55 nm; 3D). A more significant decrease in the BET surface area and micropore volume of BEA compared to that of ZSM-5 and MOR could be assigned, therefore, to a much easier diffusion of Co species into the BEA zeolite pores during the impregnation[13]. This would result in a higher Co fraction located in the BEA micropores.

The number of sites of CO adsorption in the cobalt zeolite catalysts was measured in this work by SSITKA. The SSITKA switch from ^{12}CO/He/Ne to ^{13}CO/He was realized (Figure S1, Electronic Supplementary Information-ESI) in order to determine the total number of surface sites in the catalysts containing 20% of cobalt and 0.1% of Pt supported on ZSM-5, MOR and BEA zeolites. Table 1 shows that the CO surface residence time (τ_{CO}) for the cobalt catalyst supported on silica was 5.2 s contrasting with an average residence time of 3.5 s for the cobalt counterparts supported on all zeolites. This proves stronger chemical interaction of CO with cobalt nanoparticles on silica support compared to the zeolite catalysts The concentration of reversibly chemisorbed carbon monoxide (N_{CO}) on cobalt silica supported catalysts is also higher than that for

Catalysis Science & Technology ARTICLE

View Article Online
DOI: 10.1039/C9CY02421B

the cobalt zeolite samples. The switch during the CO adsorption in the presence of hydrogen (from $^{12}CO/H_2/He/Ne$ to $^{13}CO/H_2/He$) but in the absence of FT reaction was performed for the silica and BEA supported cobalt catalysts (Table 1). The concentrations of reversibly adsorbed carbon monoxide (N_{CO}) on both samples in helium and in the presence of

hydrogen are almost the same. This suggests that at T = 100 °C there is non-competition between H_2 and CO for active sites. Hence, CO is a dominating specie on the surface of the amorphous silica and on the BEA zeolite. This observation is in agreement with previous report by Frøseth et al. [29]. However, Enger et al. [31] noticed a different trend for cobalt supported on different modified aluminas with and without promoters such as Zn, Re, Ni and Mg. The authors have found that the co-adsorption of CO with H_2 prior to the reaction showed an apparent competitive H_2-CO adsorption which resulted in a lower CO saturation coverage in hydrogen than

Table 1. Catalyst characterization and SSITKA CO adsorption data (switches between $^{12}CO/He/Ne$ and $^{13}CO/He$).

Catalyst	Co size (nm)[a]	τ_{CO} (s)	N_{CO}[b] (µmol/g)	N_{CO}[c] in H_2 presence (µmol/g)
$CoPt/SiO_2$	17.3	5.2	90	90
CoPt/ZSM-5	26.4	3.0	49.6	-
CoPt/BEA	16.2	2.9	51.1	53
CoPt/MOR	27.5	3.5	60.2	-

[a] Co = 0.75 · dCobalt oxide (nm). Determined by XRD analysis.
[b] Amount of CO adsorbed at 100°C, evaluated from SSITKA.
[c] Amount of CO adsorbed at 100 °C in presence of hydrogen, with only CO feed.

The amount of reversibly adsorbed carbon monoxide (N_{CO}) measured by SSITKA is a function of cobalt dispersion. Among the cobalt zeolite catalysts, the highest number of CO adsorption sites was detected over the mordenite-based sample. Indeed, according to our previous results[13], the Co/MOR and Co/BEA catalysts showed a significant dispersion in the pore volume after cobalt impregnation, which is related to cobalt localisation inside the zeolite micropores. The pore volume of Co/ZSM-5 is only slightly affected by impregnation. This suggests preferential location of cobalt particles on the zeolite outer surface. The nitrogen adsorption data are consistent with TEM images of the relevant catalysts[13], which also suggest preferential localisation of cobalt on the outer surface of narrow pore ZSM-5 zeolite.

Pt-promoter effects on the kinetic parameters of cobalt catalysts during FT synthesis

Figure 1(a,b) shows CO conversion as a function of time on stream over non-promoted and Pt-promoted silica supported cobalt catalysts with syngas with the H_2/CO ratio of 2 and 5.

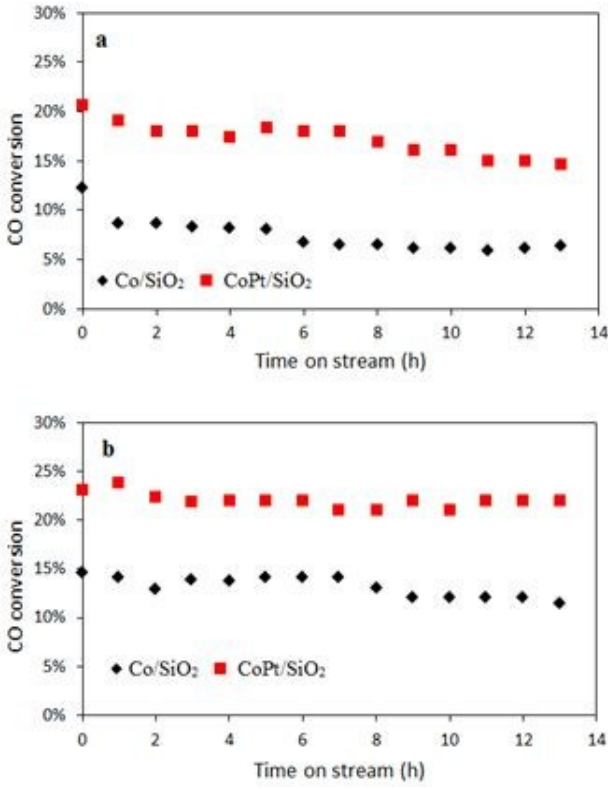

Figure 1. CO conversion as a function of time on stream for non-promoted and promoted cobalt catalysts at (a) Ratio H_2/CO=2 and (b) Ratio H_2/CO = 5. Reaction conditions: 250 °C, GHSV =

View Article Online
DOI: 10.1039/C9CY02421B

Table 2. Catalytic performance of promoted Pt and unpromoted cobalt catalysts. Reaction conditions: 250 °C, 1 atm, GHSV = 6750 h^{-1} and 9000 h^{-1}.

Catalyst	Ratio feed H_2/CO	X_{CO} (%)	S_{CH4} (%)	τ_{CO} (s)	τ_{CHx} (s)	N_{CO}[a] (µmol/g)	N_{CHx}[a] (µmol/g)	θ_{CO}[b]	θ_{CHx}[b]	TOF_{SSITKA}[c] 10^{-2} (s^{-1})	Rate[d] (µmol/g s)	R_{SSITKA}[e] (µmol/g s)
Co/SiO_2	2	6	86	2.3	19.0	38	17	nd	nd	1.8	1.1	0.9
	5	11	92	2.0	13.0	31	24	nd	nd	3.6	1.9	1.8
$CoPt/SiO_2$	2	15	85	2.8	17.0	39	35	0.43	0.39	2.9	2.5	2.1
	5	21	93	1.8	11.5	23	38	0.26	0.42	4.7	3.6	3.3

[a] $N_i = \frac{Fi_{out}}{W}\tau i$, where *W* is the catalyst loaded. (Experimental error in the number of active sites equal to 6%).
[b] Surface coverage. $\theta = N_i/N_{total.}$, (i = CO, CHx).
[c] $TOF_{FSSITKA}$ = surface coverage/surface residence time of CHx.
[d] Rate determined by GC analysis ($R = \frac{CO\ converted}{W}$).
[e] Rate determined by SSITKA analysis ($R_{SSITKA} = \frac{N_i}{\tau_i}$).

The Pt-promoted catalyst exhibits higher CO conversions with both H_2/CO ratios in syngas (Figure 1a). Similar behaviour was noticed by Jacobs et al. [3] using the Pt and Ru promoters on the alumina, titania and silica supported cobalt catalysts. For the non-promoted catalyst at H_2/CO ratio feed of 2, the CO conversion slightly decreases at the first hours of reaction. Considering the whole time on stream (around 13 h), the non-promoted catalyst lost 50% of the CO conversion, contrasting with the 30% decrease for the Pt-promoted cobalt catalyst. Increasing hydrogen partial pressure from 0.29 bar to 0.58 bar improved catalyst stability for both samples. In fact, the promoted Pt catalyst becomes completely stable with H2/CO=5 in syngas during 14 hours of reaction.

The non- promoted catalyst exhibits a slight decrease in CO conversion from 15% to 11%. The literature points out that the presence of noble metals has the ability to restrict carbon deposition and formation of cobalt support mixed oxides during FT synthesis[1,32]. The promoter effect over catalyst stability can be also associated to the type of support applied. As showed in Table 2, methane is the major product of the reaction under these conditions for both catalysts, with methane selectivity higher than 80%. Table 2 also shows the number of active sites measured by SSITKA (N_{CHx}) and the SSITKA reaction rate (RSSITKA). The RSSITKA is obtained by the division of the amount of active intermediates by its surface residence time. Note that the RSSITKA and the reaction rate that considers the amount of CO converted per gram of catalyst (Table 2) display similar values. While the number of adsorbed carbon monoxide (N_{CO}) surface species is similar for both catalysts, cobalt Pt-promoted catalysts present larger amount of intermediates leading to methane (N_{CHx}) at both H_2/CO ratios in comparison with the non-promoted samples. This result is interesting, since SSITKA studies have demonstrated, that higher coverage of CH_x intermediates could lead to higher reaction rate and high chain growth probability, which causes an increase in the selectivity toward the C_{5+} hydrocarbons and a decrease in the selectivity to methane[33,34]. Note that the lifetime of adsorbed CH_x species slightly decreases after the promotion with Pt. The higher number of CH_4 intermediates (N_{CHx}) combined with their slightly shorter lifetime (τ_{CHx}) in the promoted cobalt catalysts are responsible for 1.3 and 1.6 times higher TOF_{SSITKA} for the Pt-promoted catalyst compared to the unpromoted counterpart in the ratio of H_2/CO equal to 2 and 5, respectively. In addition, the both reaction rates also increased over the Pt-promoted catalyst. Hence, it is possible to conclude that promotion with Pt results in a significant increase in the activity. This effect is due to both the increase in the number of active sites and their intrinsic activity (TOF_{SSITKA}).

θ_{CO} and θ_{CHx} over the CoPt promoted catalysts were altered as function of the H_2 to CO ratio feed. θ_{CO} is slightly higher than θ_{CHx} at H_2/CO ratio of 2 and at ratio feed of H_2/CO equal to 5, θ_{CHx} became higher than θ_{CO} because at higher hydrogen partial pressure, more hydrogen molecules at the catalyst surface favoured the CO hydrogenation. Vasiliades et al.[27] noticed a significantly higher θ_{CO}

View Article Online
DOI: 10.1039/C9CY02421B

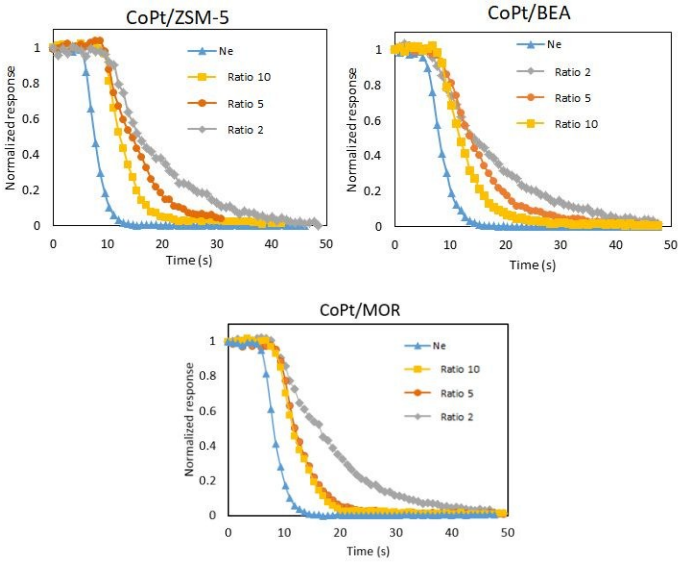

Figure 2. Transient curves of inert (Ne) and intermediates leading to CH_4 from the switch of $^{12}CO/H_2/He/Ne$ to $^{13}CO/H_2/He$ in function of ratio feed of H_2/CO (2, 5 and 10). Reaction condition: 250 °C, 1 atm, GHSV = 8 599 h^{-1}, 11 465 h^{-1} and 15 191 h^{-1}.

than θ_{CHx} over two commercial Co-based catalysts supported on carbon-cobalt and uncoated γ-Al_2O_3 catalysts for the FT synthesis. In addition, the authors observed lower total surface coverage than in the present work, which can be attributed to the longer time on stream applied in their study (32h against 3h of the present work). At longer time on stream, the presence of inactive carbonaceous species and other deactivation phenomena can modify the surface kinetic parameters and increase the lifetime of intermediates (τ_{CHx}) on the catalyst surface causing the decrease in the turnover frequency[12]

Table 2 also demonstrates the effect of the H_2/CO feed ratio. The increase in the H_2/CO feed ratio influenced the catalyst activity for both cobalt catalysts. This may be correlated to the reaction condition applied, due to the influence of Pt over FT reaction rate be more noticeable at atmospheric pressure[6,34]. The lifetime of CH_x intermediates leading to methane (τ_{CHx}) is shorter at higher H_2/CO ratio due to higher number of available hydrogen species and faster hydrogenation. Note that the rate constant determined by GC analysis at conventional steady state conditions presents similar values with the rate constant in the SSITKA experiments (Table 1).

Influence of the zeolite support on the intrinsic kinetic parameters of cobalt catalysts in CO hydrogenation

All cobalt based catalysts were reduced in hydrogen flow of 8 mL/min at 400 °C before the CO hydrogenation. Afterwards, the samples were cooled down to the reaction temperature of 250 °C.

The SSITKA measurements were done on all cobalt based catalysts at ambient pressure and after 3 h of reaction under different feed H_2/CO ratios (2, 5 and 10) corresponding to hydrogen partial pressure of 0.29 bar, 0.58 bar and 0.83 bar, respectively. Carbon monoxide conversion and methane selectivity measured at quasi-steady state reaction conditions as a function of the H_2/CO feed ratio for each catalyst are displayed in Table 3. Table 3 also shows the SSITKA data for each catalyst as functions of the H_2/CO feed ratio.

Under steady state conditions and in the range of hydrogen partial pressures, the CO conversion was higher over the cobalt catalysts supported on MOR, followed by BEA and ZSM-5. The ZSM-5 supported cobalt catalyst presented the smallest FT reaction rate. Increasing the hydrogen partial pressure in the feed affects the CO conversion over all supported catalysts. However, while the same trend is observed among the zeolites, CoPt/MOR is the most active catalyst at all H_2/CO ratio feed applied. Methane and water were the major products for all samples under applied conditions. The CO residence time (τ_{CO}) slightly decreases or even remains constant, while the CH_x residence time significantly decreases as a function of H_2 partial pressure (Table 3).

Figure 2 displays the methane and inert gas (neon) transient response curves obtained during the switch of $^{12}CO/H_2/He/Ne$ to $^{13}CO/H_2/He$ at different H_2/CO ratios. The transient curves help to understand the influence of H_2 to CO feed ratio on the catalytic activity, once faster methane transient responses were observed at

View Article Online
DOI: 10.1039/C9CY02461B

Table 3. Catalytic performance and SSITKA results (switches between $^{12}CO/H_2/He/Ne$ and $^{13}CO/H_2/He$) under different feed ratio of H_2/CO. Reaction condition: 250 °C, 1 atm, GHSV = 8 599 h^{-1}, 11 465 h^{-1} and 15 191 h^{-1}.

Catalyst	H_2/CO	X_{CO} (%)	S_{CH4} (%)	TOF_{SSITKA} 10^{-2} (s^{-1})	τ_{CO} (s)	τ_{CHx} (s)
CoPt/MOR	2	11.0	78	2.5	3.1	16.9
	5	17.0	82	4.1	2.5	12.0
	10	26.0	78	5.2	2.9	12.1
CoPt/ZSM-5	2	4.6	71	1.3	2.0	19.0
	5	6.7	87	2.0	2.0	16.6
	10	10.0	90	2.7	2.4	12.4
CoPt/BEA	2	6.4	82	1.8	2.7	17.3
	5	8.9	87	2.6	2.5	13.9
	10	16.0	75	3.7	2.3	12.1

higher partial pressures of hydrogen. Table 3 also shows that higher H_2/CO ratio in syngas results in the decrease in the residence time of CH_x intermediates, while the residence time of reversibly adsorbed CO is only slightly affected by syngas chemical composition. This observation is consistent with earlier results of Panpranot et al. [35] who observed for amorphous and mesoporous silica (MCM-41), a consistent drop of τ_{CH4} with increasing hydrogen partial pressure. On the other hand, Frøseth et al.[36] found that increasing H_2/CO ratio slightly affects the surface residence time of CH_x intermediates (τ_{CHx}).

The authors also concluded that the intrinsic site activity and concentration of surface intermediates for CO hydrogenation were strongly dependent on the hydrogen partial pressure.

The influence of the H_2/CO feed ratio for each sample on the SSITKA reaction rate (R_{SSITKA}), number of adsorbed carbon monoxide (N_{CO}) and concentration of CH_4 intermediates (N_{CHx}) is displayed in Figure 3(a,b).

Note that the total number of active sites number of molecularly adsorbed carbon monoxide molecules (N_{CO}) decreases with increasing the H_2/CO ratio for CoPt/MOR and CoPt/BEA, while the number of CH_x intermediates increases. This occurred due to higher CO conversion (see Table 3) and site competition between CO and CH_x chemisorbed intermediates. With the increase in the hydrogen partial pressure, the catalyst surface got enriched with hydrogen available to bond with the carbon atoms formed on the CO dissociation. For that reason, faster formation of CH_x intermediates resulted in lower surface lifetime of the CH_x intermediates (τCH_x) and in their faster hydrogenation to CH_4. For the cobalt catalyst supported on ZSM-5 (microporous structure), N_{CO} value remained

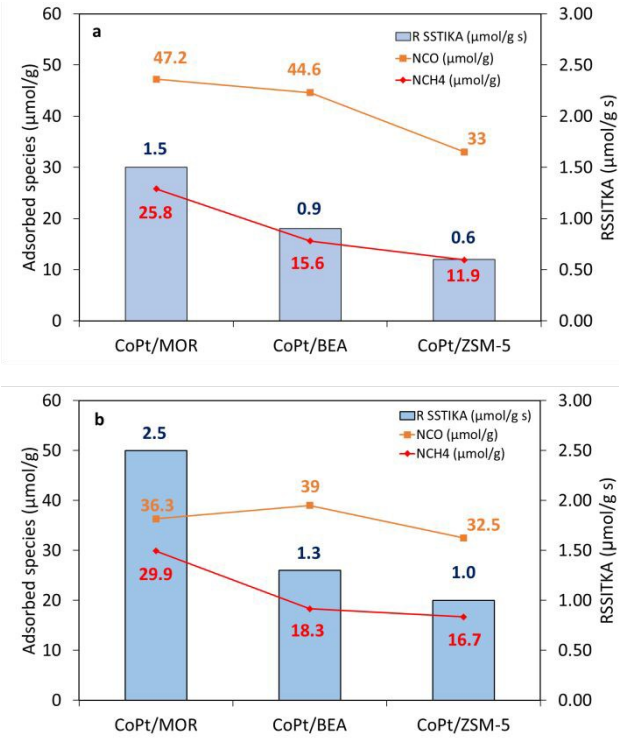

Figure 3. Number of CO sites (N_{CO}), number of CH_x sites (N_{CHx}) and SSITKA reaction rate in ratio feed of H_2/CO equal to 2 (a) and 5 (b). Reaction condition: 1 atm, 250 °C, GHSV = 8 599 h^{-1} and 11 465 h^{-1}.

constant (33 µmol/g for ratio 2; 32.5 µmol/g for ratio 5 and 33.6 µmol/g for ratio 10). Higher amount of CH_x intermediates

View Article Online
DOI: 10.1039/C9CY02421B

giving methane on their hydrogenation was observed on CoPt/MOR.

Note that the MOR zeolite showed the highest N_{CHx} among all zeolites. Interestingly, for cobalt catalyst supported on ZSM-5, N_{CO} and N_{CH4} are smallest among all samples. This is also consistent with low cobalt dispersion detected by characterization techniques in CoPt/ZSM-5[13].Our results clearly suggest that higher cobalt dispersion obtained by insertion and confinement of cobalt nanoparticles into the micropores of the MOR and BEA zeolites leads to higher concentration of the CH_x hydrogenation sites and higher FT reaction rate. This can possibly explain highest FT reaction rates observed over the catalyst supported by MOR (Figure 4).

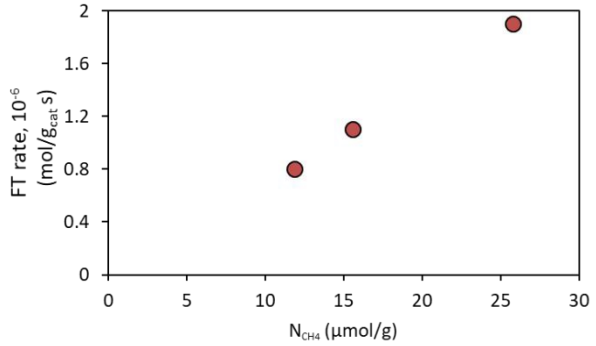

Figure 4. Correlation between FT reaction rates measured from steady state experiments and concentration of CH_4 intermediates evaluated from SSITKA. Reaction conditions: 1 atm, 250 °C, GHSV = 8 599 h^{-1} and ratio feed of H_2/CO equal to 2.

Previous DFT modelling[37] suggests that carbon monoxide molecular adsorption occurs on cobalt nanoparticle terraces, while carbon monoxide dissociation and hydrogenation to methane may involve edges of cobalt nanocrystallites. Our results did not show any noticeable increase in the intrinsic reactivity of CH_x intermediates over cobalt nanoparticles inside the zeolite micropores. It seems that the intrinsic activity of cobalt sites is not modified by their inclusion into the zeolite micropores.

The variations of N_{CO}, N_{CHx} and R_{SSITKA} as functions of the zeolite supports are consistent with cobalt localization within porous structure. According to our earlier work[38], an increase in the size of the zeolite micropore results in an increase in the amount of cobalt located inside of the pores. Since the channel diameters of BEA and MOR are larger than for ZSM-5, this leads to the fact that the micropores of ZSM-5 contain a smaller amount of cobalt available for the reaction. Most of cobalt is located on the zeolite outer surface of ZSM-5. Consequently, cobalt dispersion and amount of cobalt sites are smaller. This affects negatively the CO conversion and SSITKA kinetic parameters such as N_{CHx} and N_{CO}. The SSITKA experiments demonstrated larger number of CH_x intermediates in the CoPt/MOR and CoPt/BEA catalysts with medium micropore size relative to the CoPt/ZSM-5 catalyst with smaller pore size.

Our previous report[13] showed rather different distribution of cobalt nanoparticles between outer surface and micropores of the zeolites. For example, in cobalt catalyst supported on ZSM-5, TEM showed[13] polycrystalline zeolite particles covered by large agglomerates of cobalt nanoparticles with sizes between 100–200 nm. Therefore, there is preferential cobalt localization on the external surface of ZSM-5. The TEM images of cobalt catalyst supported on MOR demonstrated a significantly higher incorporation of cobalt nanoparticles in the zeolite crystallites. Even though, some fraction of cobalt nanoparticles was also observed on the surface of the zeolite crystals. TEM images of cobalt catalyst on BEA displayed cobalt located inside of zeolite crystals.

The low activity of cobalt catalyst supported on ZSM-5 was attributed to the preferential localization of cobalt on the outer surface of the zeolite and low concentration of active sites because of poor cobalt dispersion. The long lifetime of the CH_x intermediates (τ_{CHx}) also contributed for the lower activity of CoPt/ZSM-5 zeolite. A more uniform distribution of cobalt between outer surface and micropores of the CoPt/MOR and CoPt/BEA catalysts results in higher FT reaction rate. Importantly, a higher FT reaction rate measured at the quasi steady state conditions coincides with a higher fraction of CH_x intermediates (Figures 3 and 4) and not to the higher concentration of molecularly adsorbed carbon monoxide molecules (N_{CO}). This is consistent with previous reports[19] and indicates that CH_x hydrogenation can be a kinetically relevant step of CO hydrogenation under these conditions. N_{CHx}, that is a measure of the concentration of intermediates able to form hydrocarbons, seems to correlate to the overall activity of the cobalt zeolite catalysts at high pressure FT synthesis. Subramanian et al. [13], using the same samples for FT synthesis under high pressure test (P=20 bar) also observed that catalytic performance was strongly affected by the type of zeolite. CoPt/MOR showed the highest CO conversion at low and high pressures among all catalysts studied.

Cobalt catalysts supported on silica and on zeolites have shown different selectivities for the C_{12+} hydrocarbons in comparison with the short-chain C_5–C_{12} paraffins at realistic FT reaction conditions [13]. The CoPt/MOR catalyst demonstrated a somewhat lower activity in the isomerization of short-chain hydrocarbons probably due to the partial neutralization of zeolite Brönsted acid sites in the 1D channels of the MOR pores by cobalt cations. In ZSM-5, cobalt is mostly located on the external surface of the zeolite crystals. Therefore, FT synthesis occurs over cobalt sites on the zeolite external surface and that only short-chain hydrocarbons can diffuse and isomerize effectively inside the pores of ZSM-5 zeolite. Because of stronger acidity compared to other zeolites, CoPt/ZSM-5 exhibited a higher activity towards the isomerization of C_5–C_{12} hydrocarbons. The trend was different for larger molecules, where isomerization activity was hindered by hydrocarbon diffusion inside the narrow ZSM-5 zeolite pores.

Conclusion

This work elucidated the roles of promotion with Pt and localization of cobalt nanoparticles within BEA, MOR and ZSM-5 zeolites on the number and intrinsic activity of active sites for CO hydrogenation using SSITKA. Platinum promotion results in the increase in both the number of active sites for CH_x hydrogenation and in their higher intrinsic activity (TOF_{SSITKA}).

In the cobalt zeolite catalysts promoted with platinum, the number of active sites is a function of cobalt distribution between the zeolite outer surface and zeolite micropores. Larger amounts of active sites and higher FT reaction rates are observed over the cobalt-mordenite catalyst with more uniform distribution of cobalt species within zeolite crystallites. The intrinsic activity of cobalt surface sites is almost unaffected by their localization in either on the zeolite outer surface or in the micropores.

The FT reaction rate at steady state conditions both under atmospheric and high pressures correlates with the amount of CH_x surface intermediates. Furthermore, the rise of hydrogen partial pressure resulted in a decline of surface residence time and an increase in the concentration of surface CH_x intermediates producing methane on hydrogenation.

Experimental

Catalyst preparation and characterization

Cobalt catalysts supported on silica with and without platinum (20 wt. % Co and 0.1 wt. %% Pt) have been synthesized by incipient wetness impregnation of commercial amorphous silica (CARIACT Q-10, Fuji Silysia) with aqueous solutions of cobalt nitrate ($Co(NO_3)_2{\cdot}6H_2O$) and tetramine platinum nitrate ($Pt(NH_3)_4(NO_3)_2$). The cobalt catalysts supported on zeolites (ZSM-5, BEA, MOR) have been synthesized by incipient wetness impregnation using the same precursors and weight contents of cobalt and platinum used for cobalt supported on silica. The ZSM-5, MOR and BEA zeolites with the Si/Al ratio of 13, 8 and 9 have been provided by Zeolyst. The catalysts were dried for 1 h at 100 °C and calcined at 450 °C in air flow of 10 mL/min for 7 h.

SSITKA and steady state catalytic tests

In all the experiments, 40 mg of catalyst was mixed with 80 mg of SiC. The samples were loaded into a millimetric fixed bed reactor (d_{in} = 2 mm) and reduced in pure H_2 flow of 8 cm^3/min for 2 h at 400 °C with a 5 °C/min heating rate. In the CO adsorption study, after reduction, the sample were cooled down in the same rate ramp to 100 °C and switches from ^{12}CO/He/Ne to ^{13}CO/He were applied to determine the total number of active sites. To evaluate both the effect of support structure and hydrogen partial pressure, the samples were submitted to the reaction temperature of 250 °C. The catalytic experiments were conducted at different ratios of H_2/CO (2, 5 and 10) in syngas with the gas hourly space velocities (GHSV) varying from 6750 h^{-1} to 15 191 h^{-1}. Then, after 3 h of reaction with the catalysts at steady-state conditions, the switches from $^{12}CO/H_2$/He/Ne to $^{13}CO/H_2$/He were applied.

Carbon monoxide conversion and reaction selectivities were determined by analysing the reaction effluents with a Shimadzu 2014 gas-chromatograph equipped with a CP-PoraPLOT and a CTR-1 column, as well as FID and TCD detectors. Nitrogen was used as an internal standard for calculating carbon monoxide conversion. The SSITKA apparatus has been described in detail in our previous reports [12,39]. It is composed of two independent gas feed lines (Figure S2, ESI). The first line is dedicated to unlabelled compounds and a tracer (CO, H_2, He, and Ne), and the second one to the isotope-labelled compounds (^{13}CO in this case). The experiment consists of a sudden replacement of one reactant by its labelled counterpart without any modification of the reaction total pressure, flow or reactant chemical composition, while an inert tracer is also

abruptly removed from the feed. The details of calculation of the number of CO and CH_x surface intermediates and TOF are given in ESI.

Acknowledgements

A. Carvalho is thankful to International Cooperation Program CAPES/COFECUB Foundation funded by CAPES – Brazilian Federal Agency for Support and Evaluation of Graduate Education within the Ministry of Education of Brazil for providing him a PhD stipend. The authors acknowledge financial support of the French National Research Agency (DirectSynBioFuel, Ref. ANR-15-CE06-0004 and NANO4-FUT, Ref. ANR-16-CE06-0013).

Conflicts of interest

There are no conflicts to declare.

References

1 F. Diehl and A. Y. Khodakov, *Oil Gas Sci. Technol.*, , DOI:10.2516/ogst:2008040.
2 S. Storsæter, Borg, E. A. Blekkan and A. Holmen, *J. Catal.*, 2005, **231**, 405–419.
3 G. Jacobs, T. K. Das, Y. Zhang, J. Li, G. Racoillet and B. H. Davis, *Appl. Catal. A Gen.*, 2002, **233**, 263–281.
4 N. Tsubaki, S. Sun and K. Fujimoto, *J. Catal.*, 2001, **199**, 236–246.
5 W. Chu, P. A. Chernavskii, L. Gengembre, G. A. Pankina, P. Fongarland and A. Y. Khodakov, *J. Catal.*, 2007, **252**, 215–230.
6 D. Schanke, S. Vada, E. A. Blekkan, A. M. Hilmen, A. Hoff and A. Holmen, *J. Catal.*, 1995, 156, 85–95.
7 G. E. Batley, A. Ekstrom and D. A. Johnson, *J. Catal.*, 1974, **34**, 368–375.
8 S. A. Gardezi, L. Landrigan, B. Joseph and J. T. Wolan, *Ind. Eng. Chem. Res.*, 2012, **51**, 1703–1712.
9 T. Fu and Z. Li, *Chem. Eng. Sci.*, 2015, **135**, 3–20.
10 S. Bai, C. Huang, J. Lv and Z. Li, *Catal. Commun.*, 2012, **22**, 24–27.
11 A. Dinse, M. Aigner, M. Ulbrich, G. R. Johnson and A. T. Bell, *J. Catal.*, 2012, **288**, 104–114.
12 A. Carvalho, V. V. Ordomsky, Y. Luo, M. Marinova, A. R. Muniz, N. R. Marcilio and A. Y. Khodakov, *J. Catal.*, 2016, **344**, 669–679.
13 V. Subramanian, V. L. Zholobenko, K. Cheng, C. Lancelot, S. Heyte, J. Thuriot, S. Paul, V. V. Ordomsky and A. Y. Khodakov, *ChemCatChem*, 2016, **8**, 380–389.
14 J. Kang, K. Cheng, L. Zhang, Q. Zhang, J. Ding, W. Hua, Y. Lou, Q. Zhai and Y. Wang, *Angew. Chemie - Int. Ed.*, 2011, **50**, 5200–5203.
15 S. L. Shannon and J. G. Goodwin, *Chem. Rev.*, 1995, **95**, 677–695.
16 J. Yang, D. Chen and A. Holmen, *Catal. Today*, 2012, **186**, 99–108.
17 V. V. Ordomsky, A. Carvalho, B. Legras, S. Paul, M. Virginie, V. L. Sushkevich and A. Y. Khodakov, *Catal. Today*, 2016, **275**, 84–93.
18 J. Van De Loosdrecht, I. M. Ciobîca, P. Gibson, N. S. Govender, D. J. Moodley, A. M. Saib, C. J. Weststrate and J. W. Niemantsverdriet, *ACS Catal.*, 2016, **6**, 3840–3855.
19 N. S. Govender, M. H. J. M. de Croon and J. C. Schouten, *Appl. Catal. A Gen.*, 2010, **373**, 81–89.
20 N. Lohitharn and J. G. Goodwin, *J. Catal.*, 2008, **257**, 142–151.
21 B. Jongsomjit, J. Panpranot and J. G. Goodwin, *J. Catal.*, 2003, **215**, 66–77.
22 H. A. J. Van Dijk, J. H. B. J. Hoebink and J. C. Schouten, *Chem. Eng. Sci.*, 2001, **56**, 1211–1219.
23 M. Rothaemel, K. F. Hanssen, E. A. Blekkan, D. Schanke and A. Holmen, *Catal. Today*, 1997, **38**, 79–84.
24 H. A. J. Dijk van, Technische Universiteit Eindhoven, 2001.
25 A. M. Efstathiou, J. T. Gleaves and G. S. Yablonsky, in *Characterization of Solid Materials and Heterogeneous Catalysts: From Structure to Surface Reactivity*, eds. M. Che and J. C. Vedrine, 2012, chapter 22, pp. 1013–1073.
26 S. Rane, Ø. Borg, J. Yang, E. Rytter and A. Holmen, *Appl. Catal. A Gen.*, 2010, **388**, 160–167.
27 M. A. Vasiliades, C. M. Kalamaras, N. S. Govender, A. Govender and A. M. Efstathiou, *J. Catal.*, 2019, **379**, 60–77.
28 X. K. Phan, J. Yang, H. Bakhtiary-Davijnay, R. Myrstad, H. J. Venvik and A. Holmen, *Catal. Letters*, 2011, **141**, 1739–1745.
29 V. Frøseth, S. Storsæter, Ø. Borg, E. A. Blekkan, M. Rønning and A. Holmen, *Appl. Catal. A Gen.*, 2005, **289**, 10–15.
30 K. F. Hanssen, E. A. Blekkan, D. Schanke and A. Holmen, *Stud. Surf. Sci. Catal.*, 1997, **109**, 193–202.
31 B. C. Enger, V. Froseth, J. Yang, E. Rytter and A. Holmen, *J. Catal.*, 2013, **297**, 187–192.
32 B. Jongsomjit, J. Panpranot and J. G. Goodwin, *J. Catal.*, 2001, **204**, 98–109.
33 J. P. Den Breejen, A. M. Frey, J. Yang, A. Holmen, M. M. Van Schooneveld, F. M. F. De Groot, O. Stephan, J. H. Bitter and K. P. De Jong, *Top. Catal.*, 2011, **54**, 768–777.
34 C. Ledesma, J. Yang, D. Chen and A. Holmen, *ACS Catal.*, 2014, **4**, 4527–4547.
35 J. Panpranot, J. G. Goodwin and A. Sayari, *J. Catal.*, 2003, **213**, 78–85.
36 V. Frøseth and A. Holmen, *Top. Catal.*, 2007, **45**, 45–50.
37 S. Shetty, A. P. J. Jansen and R. A. van Santen, *J. Am. Chem. Soc.*, 2009, **131**, 12874–12875.
38 A. Carvalho, M. Marinova, N. Batalha, N. R. Marcilio, A. Y. Khodakov and V. V. Ordomsky, *Catal. Sci. Technol.*, 2017, **7**, 5019–5027.
39 B. Legras, V. V. Ordomsky, C. Dujardin, M. Virginie and A. Y. Khodakov, *ACS Catal.*, 2014, **4**, 2785–2791.